Transparent hybrid inorganic/organic barrier coatings for plastic organic light-emitting diode substrates

Tae Won Kim,[a] Min Yan, Ahmet Gün Erlat, Paul A. McConnelee, Mathew Pellow, John Deluca, Thomas P. Feist, and Anil R. Duggal
General Electric Global Research Center, Schenectady, New York 12309

Marc Schaepkens
General Electric Advanced Materials, Strongsville, Ohio 44149

(Received 4 January 2005; accepted 14 March 2005; published 27 June 2005)

We have developed a coating technology to reduce the moisture permeation rate through a polycarbonate plastic film substrate to below 1×10^{-5} g/m^2/day using plasma-enhanced chemical vapor deposition. Unlike other ultrahigh barrier (UHB) coatings comprised of inorganic and organic multilayers, our UHB coating comprises a graded single hybrid layer of inorganic and organic materials. Hardness and modulus of the inorganic and the organic materials are tailored such that they are similar to those of typical glass-like materials and thermoplastics, respectively. In this barrier structure, the composition is periodically modulated between the inorganic and the organic materials, but instead of having distinctive interfaces between two materials, there are "transitional" zones where the coating composition changes continuously from one material to another. Our UHB coating also has superior visible light transmittance and color neutrality suitable for the use of display and lighting device substrates. © *2005 American Vacuum Society.*
[DOI: 10.1116/1.1913680]

I. INTRODUCTION

The use of plastic film substrates enables fabrication of new applications in the area of flexible opto-electronics, such as flexible display and lighting, using low-cost roll-to-roll fabrication technologies. One major limitation of bare plastic film substrates in these applications is the rapid oxygen and moisture diffusion through the substrates and subsequent moisture and oxygen induced degradation of the opto-electronic devices. Thus, it is imperative for the plastic substrate to have hermetic coatings to prevent moisture and oxygen permeation.[1–6] There has accumulated a great amount of literature over the last 20 years on applying vacuum-deposited inorganic layers on plastic substrates in order to improve the barrier properties against water vapor and oxygen permeation.[7–11] Although bulk inorganics such as a perfect SiO_2 film are effectively impermeable to moisture and oxygen,[12,13] single-layer inorganic barrier coatings reduce the moisture and oxygen permeation rates by at most two to three orders of magnitude as compared to those through the uncoated plastic.[9,10,14–16] The reason for the limited barrier improvement attainable with a single inorganic barrier coating is now well understood to be due to nanometer- to micron-sized defects in the coating that originate either from the surface roughness of the underlying substrate or from the inorganic coating processing conditions.[17] These defects provide easy pathways for moisture and oxygen diffusion, and thus limit the barrier performance. Evidence of this defect-driven permeation mechanism can be found through studies of permeation rate as a function of inorganic coating thickness. Permeation rate through a defect-free bulk film should exhibit Fickian diffusion and should thus vary inversely with film thickness. However, this is not normally observed for thin-film barrier coatings. Typically, the gas permeation rate reduces rapidly by two to three orders of magnitude with increasing coating thickness up to a "critical thickness" of 10–30 nm but, for larger thicknesses, the permeation rate does not decrease further.[10,16] Thus, regardless of barrier material or deposition method, the best barrier performance from a single-layer inorganic coating is several orders of magnitude short of the organic light-emitting diode (OLED) requirement.

In order to meet the stringent requirements put forth for the design of OLEDs and other organic electronic devices on plastic substrates, a robust coating design should be realized that avoids the hindrance of barrier improvement by defects. Multilayer barrier structures comprised of multiple sputter-deposited aluminum oxide inorganic layers separated by polymer multilayer (PML) processed organic layers have demonstrated promising moisture permeation rates in the range of 10^{-6}–10^{-5} g/m^2/day.[18–20] It is commonly understood that organic layers decouple the defects in the inorganic layers and thus prevent their propagation from one inorganic layer to the other.[21] A modeling study suggests that this defect decoupling due to the organic/inorganic multilayers forces a tortuous path for moisture and oxygen diffusion, and thus reduces the permeation rate by several orders of magnitude.[16] Another study suggests that the inorganic/organic multilayer stack leads to higher performance through a transient rather than steady-state phenomenon.[22] Regardless of mechanism, this multilayer barrier stack approach appears to be capable of yielding the required level of performance for OLED applications.

[a]Current address: General Electric Advanced Materials, Strongsville OH 44149; electronic mail: taewon.kim@ge.com

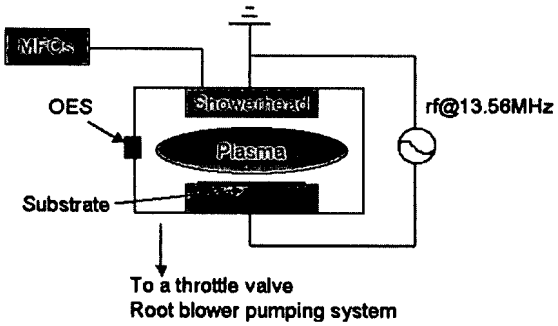

FIG. 1. The schematic of the plasma reactor.

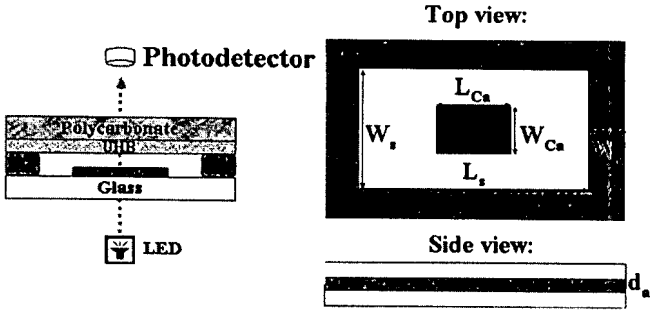

FIG. 2. Illustration of the calcium corrosion test setup and the test cell geometry.

One potential limitation of the multilayer stack approach is that this type of structure tends to suffer from poor adhesion and delamination, especially during the thermal cycles of the OLED fabrication processes, since the inorganic and organic layers have sharp interfaces with weak bonding structure due to the nature of the sputter deposition and PML processes.[23,24] In order to overcome this, we have developed a graded ultrahigh barrier (UHB) coating using plasma-enhanced chemical vapor deposition (PECVD) that can effectively stop defects from propagating through the coating thickness. In this article, we describe the fabrication of the UHB coating in a parallel plate capacitively coupled plasma reactor and its properties, including barrier performance and optical transparency.

II. EXPERIMENTS

A. PECVD reactor

The experiments were conducted in a commercially available parallel plate capacitively coupled plasma reactor (Plasmatherm 790) shown schematically in Fig. 1.[16] This type of reactor is commonly used to etch polysilicon or deposit thin films. This reactor is equipped with optical emission spectrometer (Ocean Optics USB2000) to monitor the optical emissions from the plasma during the process. Radio frequency power in the range of 100–500 W at 13.56 MHz is capacitively coupled to plasma through a bottom electrode. The electrode and reactor walls were kept constant at 55 °C by a cooling system. Gas flow into the reactor is controlled by mass flow controllers (MFCs). The gases enter the reactor through the showerhead 1 in. above the bottom electrode, and are pumped by a 270 m^3/h root blower pump package. The reactor base pressure is below 10 mTorr and typical operating pressure is between 100 and 1000 mTorr. The reactor pressure is controlled by a variable position butterfly valve. The 125 μm thick high heat polycarbonate films were cut into pieces, each 200 mm in diameter, which were framed between two aluminum rings for the ease of handling, and placed on the bottom electrode.

B. Ca corrosion test

One major obstacle in developing the UHB coatings is the lack of a readily available measurement system for the water vapor transmission rate (WVTR) in the range of $10^{-5}-10^{-6}$ $g/m^2/day$. In this study, a WVTR measurement system was built based principally on the degradation of Ca as it reacts with water vapor.[25,26] The schematics of a calcium cell, the measurement system, and the cell geometry are shown in Fig. 2. As water vapor and oxygen permeate through the substrate and/or the edge perimeter seal, or are being released from any internal sources (e.g., residual moisture in adhesive), they react with calcium inside the cell according to the following reactions:[26,27]

$$Ca + 2H_2O \rightarrow Ca(OH)_2 + H_2, \tag{1}$$

$$2Ca + O_2 \rightarrow 2CaO. \tag{2}$$

It has been shown in a similar technique that oxidation would account for less than 5% of the calcium degradation.[26] Therefore, reaction (1) is predominant. As water vapor permeation progresses, the calcium layer becomes thinner and more transparent. Since the optical density (OD) of a film is proportional to its thickness, WVTR can be calculated using

$$\mathrm{WVTR} = -2A\frac{M[H_2O]}{M[Ca]}\rho_{Ca}\frac{L_{Ca}W_{Ca}}{L_sW_s}\frac{d(\mathrm{OD})}{dt}, \tag{3}$$

where A is the scaling factor between calcium thickness and OD, $M[H_2O]$ and $M[Ca]$ are the molar masses of water and Ca with values of 18 and 40.1 amu, respectively; ρ_{Ca} is the density of calcium; L_{Ca} and W_{Ca} are the length and width, respectively, of the deposited Ca; L_s and W_s are the respec-

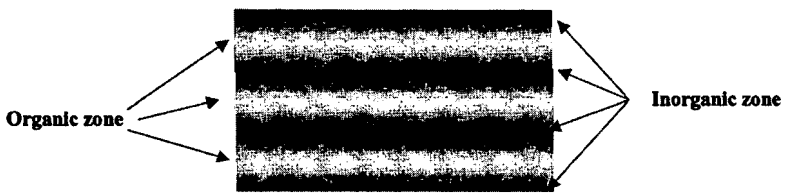

FIG. 3. The schematic of the graded inorganic/organic UHB coating.

TABLE I. Conditions of two base PECVD processes and material properties.

	Inorganic process	Organic process
Precursors	SiH_4 (2% in He)	SiC_xH_y
	NH_3	(C weight % >50%)
	O_2	Ar
Flow rate (sccm)	20–500	50–100
Pressure (mTorr)	100–1000	100–1000
rf power (W)	100–400	100–400
Film hardness (GPa)	10–15	<1
Film modulus (GPa)	100–500	<10
Film $\%T$	>95%	>95%
Deposition rate (nm/min)	40–60	40–80

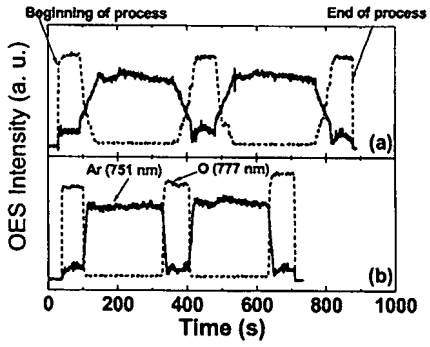

FIG. 5. Time-resolved optical emission spectra for the PECVD graded UHB processes with (a) 40 nm and (b) 5 nm of the "transitional" zone thickness.

tive length and width of the permeation area defined by the interior boundary of the edge perimeter seal (Fig. 2), and $d(OD)/dt$ is the slope of the measured optical absorbance as a function of time. More details of the calcium test cell fabrication and testing procedures have been described elsewhere.[28]

III. RESULTS AND DISCUSSION

The UHB coating consists of a graded single hybrid layer made up of inorganic and organic materials as schematically shown in Fig. 3. In this barrier structure, the organic materials effectively decouple defects growing in the normal direction to the film but, instead of having a sharp interface between inorganic and organic materials, there are "transitional" zones where the coating composition varies continuously from inorganic to organic and vice versa. These "transitional" zones bridge inorganic and organic materials, resulting in a single layer structure with improved mechanical stability and stress relaxation,[21] relative to that of multilayer barrier structures.

A. Fabrication of graded UHB coating

There are two base PECVD processes required to fabricate the UHB coating: an inorganic and an organic process. The inorganic process utilizes a combination of silane (2% silane diluted in He), ammonia, and oxygen gases to create a material composition ranging between silicon nitride and silicon oxide. The organic process includes a combination of organosilicon precursor and Ar gases to create a Si-containing organic material. The inorganic and the organic processes were tailored such that the resulting materials have similar hardness and elastic modulus to those of glass-like materials and thermoplastics, respectively. Table I summarizes the process conditions and material properties. Hereafter, the inorganic and the organic materials are defined as those deposited with 0% and 100% organic precursor concentration, respectively. The composition of the inorganic material (0% organic precursor) and the organic one (100% organic precursor) can be found in Fig. 4.

Although PECVD inorganic film, such as silicon oxide and aluminum oxide, deposited on organic materials by nature has tens of nanometers thick "transitional" regions that exhibit a continuously graded composition between inorganic and organic materials due to ion bombardment,[21] high energy ion bombardment normally results in a highly stressed film, which adversely affects the adhesion of subsequent layers. For instance, OLED devices typically require the deposition of a transparent conductive oxide electrode such as indium tin oxide on top of the UHB. A low stress

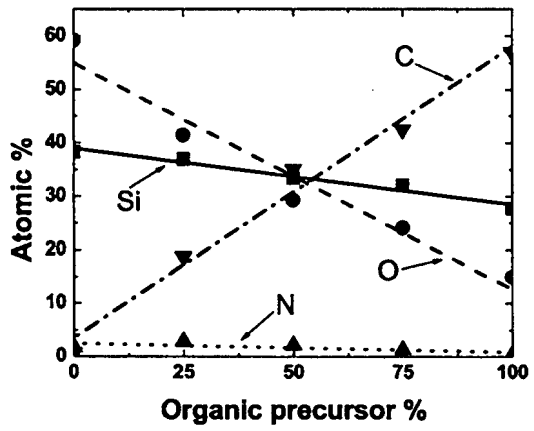

FIG. 4. XPS analyses on the coating composition as a function of precursor gas composition.

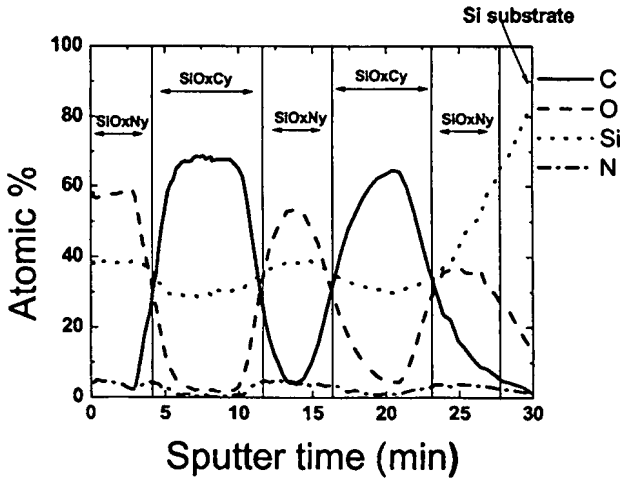

FIG. 6. Depth-profile XPS spectrum for the graded inorganic/organic UHB coating.

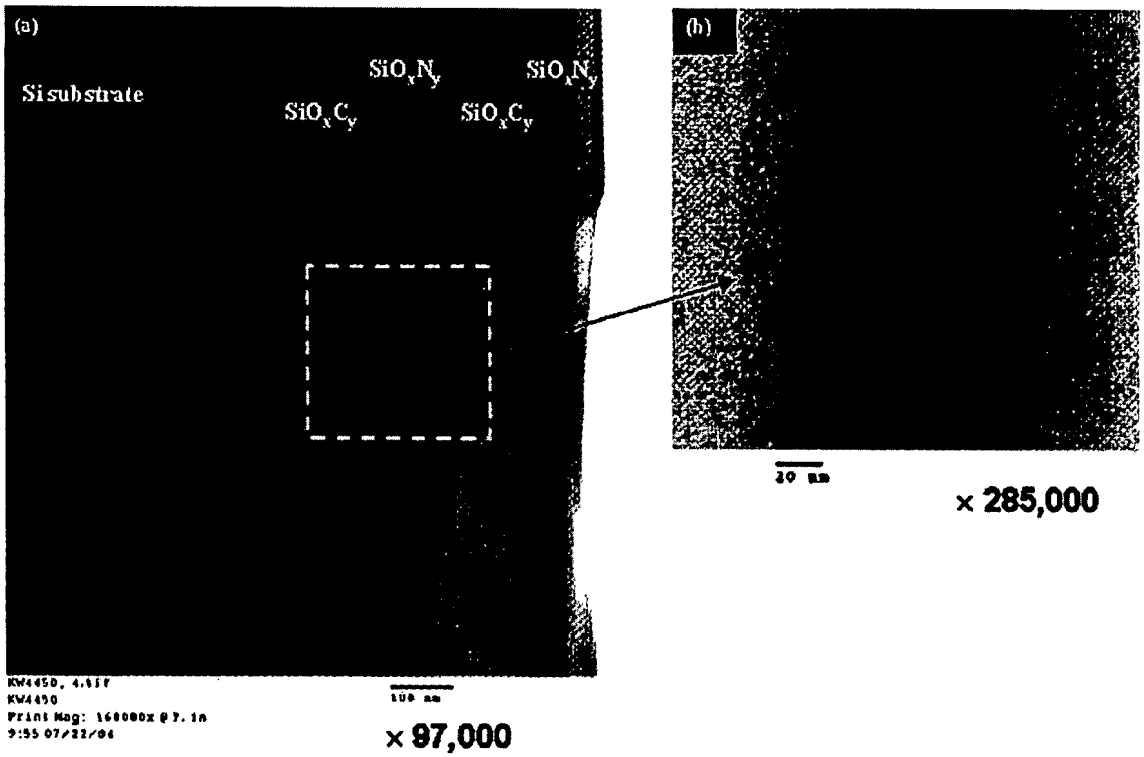

FIG. 7. Cross-sectional TEM images of the graded UHB coating with (a) low magnification and (b) high magnification.

barrier coating is desirable for better adhesion of this layer. Thus, instead of resorting to high ion bombardment energy, our graded UHB structure is obtained by gradually mixing the inorganic and the organic processes. At constant pressure and rf power, each mass flow controller for individual process gases is programmed to achieve continuous compositional changes, while the plasma remains on, in order to achieve a gradual change in the coating composition from inorganic to organic materials and vice versa. For example, if one wants to achieve a coating composition that comprises 90% inorganic and 10% organic materials, MFC values for the inorganic and the organic process gases are set at 90% and 10% with respect to their original values, respectively. The thickness of the "transitional" zone is determined by the time to change the precursor gas composition from the inorganic process to the organic one and vice versa. Typically, due to the nonlinearity of the plasma process, mixing of precursors for two different processes often results in unexpected coating compositions unless the process conditions are carefully selected. In order to prevent this possibility, the inorganic and the organic processes were developed at the same pressure and rf power. In addition, the inorganic and the organic processes were optimized to have comparable deposition rates.

In order to ensure that coatings with mixed organic and inorganic compositions could be deposited by keeping all PECVD process variables constant and by changing only the gas composition, coatings deposited from selected gas combinations were analyzed. Figure 4 shows the results of x-ray photoelectron spectroscopy (XPS) analysis of these coatings. For these measurements, the coatings were deposited onto a silicon substrate and a few monolayers of the coating were removed from the top surface by low energy Ar sputtering to eliminate surface contamination. Figure 4 indicates that a linear change in the coating composition can be achieved with a linear change in the precursor gas composition. For example, the carbon concentration is nearly zero when the precursor gas composition is that of the pure inorganic process, and increases linearly with increasing percentage of the organic precursor. Note that the precursor gases for the organic process do not contain oxygen; the oxygen present in the 100% organic process is due to desorption from the reactor and/or oxidation of the organic coating at the atmosphere.

Based on these results, processes were developed to create a single coating with the graded structure depicted in Fig. 3 and varying thickness of the "transitional" zones between inorganic and organic materials. Figures 5(a) and 5(b) compare the time-resolved optical emission spectra obtained during processing for two different processes with planned "transitional" zones of 40 and 5 nm, respectively. For these measurements, representative emission lines (O at 777 nm for the inorganic process and Ar at 751 nm for the organic process) were selected to monitor the precursor composition change during the UHB deposition. The plasma was on for the whole time at constant pressure and rf power during the process. Figure 5 clearly indicates that a continuous change in the plasma composition is achieved during both UHB processes. The O emission intensity that represents the inorganic precursor fraction is high during the inorganic process, and decreases continuously towards a baseline when the fraction of the organic process gases monotonically increases during

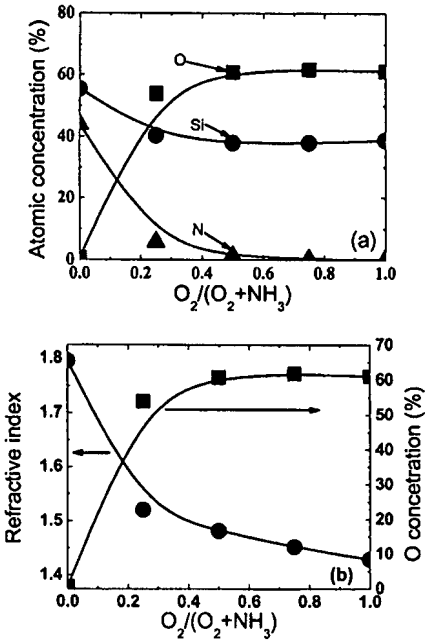

FIG. 8. (a) Coating composition and (b) the refractive index at 550 nm of the inorganic material as a function of oxygen flow rate.

the "transitional" zone process. At the same time, the Ar emission intensity that represents the organic precursor fraction increases continuously.

In order to verify that the desired graded composition coatings were made, depth-profile XPS measurements and cross-sectional transmission electron microscopy (TEM) were performed on the final coatings. The depth-profile XPS analysis for the 40 nm transition zone sample shown in Fig. 5(a) is shown in Fig. 6. The data clearly suggest a continuous change in composition as a function of sputter time and hence depth. The XPS depth profiling was accomplished with low energy Ar sputtering. However, there is still the possibility that the apparently continuous change in composition observed may be an artifact caused by chemical changes of the surface induced by mixing or preferential sputtering of the elements.[23] In order to eliminate this interpretation, cross-sectional TEM analysis was performed in parallel on the same coating. Figure 7 shows representative TEM images. The images clearly depict a graded structure without a discrete interface.

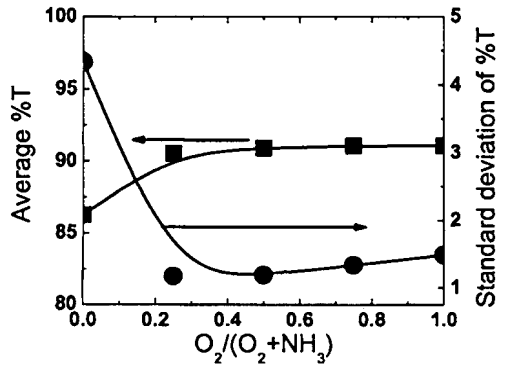

FIG. 9. The overall visible light transmittance and its standard deviation of the graded UHB coating as a function of oxygen flow rate in the inorganic process.

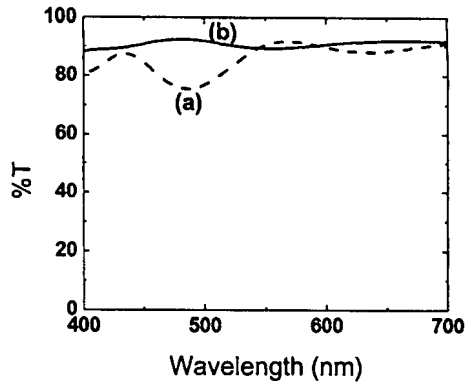

FIG. 10. The complete $\%T$ spectra through two distinctive UHB coatings: (a) silicon nitride as the base inorganic material (oxygen flow fraction of 0), and (b) silicon oxynitride as the base inorganic material (oxygen flow fraction of 0.25).

B. Refractive index matched UHB

Superior light transmittance and color neutrality is another critical substrate requirement for optoelectronic devices such as OLEDs. One issue with the multilayer approach to a UHB is that the separate organic and inorganic layers typically have different indices of refraction. This leads to multiple reflections and usually additional loss of optical transmission through the multilayer stack. One way around this is to engineer the thickness of the layers to create an interference effect that improves light transmission. Unfortunately, the optimal thicknesses for optical performance are usually not the optimal thicknesses for barrier performance, so that overall coating optimization involves an undesirable tradeoff.[16,21]

The single graded layer UHB approach can circumvent this tradeoff. In particular, since PECVD is utilized to deposit both inorganic and organic materials, there is a large freedom to tailor film properties such as refractive index through film composition. Thus, it is possible to develop a process that yields the same refractive index for both the organic and inorganic materials and hence avoid multiple reflections. We chose to do this by modifying the inorganic material such that its index matched that of the organic one ($n \sim 1.5$).

Figures 8(a) and 8(b) show the coating composition and refractive index of the inorganic material at 550 nm as a function of oxygen flow rate. The inorganic coatings were deposited on a Si chip at various oxygen flow rates while total flow rate was maintained at a constant value. The coating composition was obtained using XPS and the refractive index was obtained using spectroscopic ellipsometry. One can see that the atomic oxygen concentration increases rapidly with a small addition of oxygen in the precursor gases, and simultaneously refractive index dramatically decreases from ~1.8 (silicon nitride) to ~1.5 (silicon oxynitride). Atomic oxygen concentration then increases slowly and

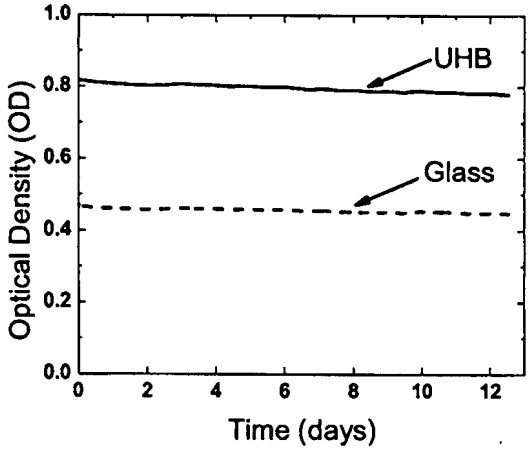

FIG. 11. Optical density vs time plots for the UHB and glass/glass reference cells, obtained from the calcium corrosion test.

finally saturates with a further increase in oxygen flow rate, and refractive index decreases slowly to ~1.4 (silicon oxide).

In order to test the overall effect of these inorganic process changes, the UHB coatings were deposited onto the polycarbonate films with the various oxygen flow rates for the inorganic process and the overall light transmittance (*%T*) through the coated films was collected using a UV-Vis spectrometer. An average *%T* and its standard deviation were calculated over the wavelength range of 400–700 nm to assess the optical transparency and the amplitude of any interference effects, respectively. Figure 9 shows these parameters as a function of oxygen flow rate. Note that the average *%T* is ~86% when the UHB coating includes silicon nitride as an inorganic material, but it increases to above 90% as the oxygen flow rate in the inorganic process increases. One can also see that the amplitude of interference is at a minimum when the oxygen flow fraction is ~0.2, where the refractive index of the inorganic material matches that of the organic material. Figure 10 compares the complete *%T* spectra through two distinctive UHB coatings: (a) silicon nitride as the base inorganic material (oxygen flow fraction of 0), and (b) silicon oxynitride as the base inorganic material (oxygen flow fraction of 0.25). One can see that with the given silicon oxynitride as the inorganic material, the single layer graded barrier coating on the polycarbonate substrate indeed has higher overall transmission and greatly minimized interference fringes relative to that with silicon nitride as the base inorganic material. This demonstrates that highly transmissive and essentially color neutral barrier coatings can be made with our single layer graded approach to an UHB.

C. Ultrahigh barrier performance

The graded UHB coating with planned 40 nm thick "transitional" zones shown in Fig. 5(a) was fabricated on the polycarbonate substrate, and the test cells along with glass/glass reference cells were prepared as depicted in Fig. 3. The Ca corrosion test was performed at 25 °C and 50% relative humidity. Figure 11 shows selected OD changes through (a) the UHB and (b) the glass/glass reference cells as a function of time, from which WVTR values of 8.6 (±0.3) $\times 10^{-6}$ g/m^2/day for the UHB and 5.9 (±0.5) $\times 10^{-6}$ g/m^2/day for the glass/glass reference cell were calculated using Eq. (3). Note that since glass is effectively a perfect barrier, WVTR of the glass/glass reference cell represents the moisture permeation through the edge perimeter seals.

IV. SUMMARY AND CONCLUSIONS

We have developed an ultrahigh barrier coating of a graded single hybrid layer made up of inorganic and organic materials using PECVD. In this barrier structure, the composition of the coating modulates periodically between the inorganic and the organic materials. The organic material effectively prevents the propagation of the defects in the coating, and thus improves the barrier performance by several orders of magnitude as compared to that of a single layer inorganic coating. In this barrier structure, however, instead of having a distinctive interface between inorganic and organic materials, there are "transitional" zones where the coating composition varies continuously from inorganic to organic and vice versa. These "transitional" zones bridge inorganic and organic materials resulting in a single-layer structure. In addition, the refractive index of the inorganic material was engineered to match that of the organic material that one can avoid multiple reflections and thus obtain superior visible light transmittance. The moisture permeation rate of the polycarbonate substrate with the UHB coating measured by the Ca corrosion test is less than 1 $\times 10^{-5}$ g/m^2/day, meeting the stringent OLED substrate requirements.

ACKNOWLEDGMENTS

This work was supported in part by the USDC/ARL program (Grant MDA972-93-2-0014). The authors would like to thank John J. Chera and Michael Larsen for the thin film characterizations.

[1]A. R. Duggal, J. J. Shiang, C. M. Heller, and D. F. Foust, Appl. Phys. Lett. **80**, 3470 (2002).
[2]A. R. Duggal, D. F. Foust, W. F. Nealon, and C. M. Heller, Appl. Phys. Lett. **82**, 2580 (2003).
[3]J. K. Mahon, J. J. Brown, T. X. Zhou, P. E. Burrows, and S. R. Forrest, 42nd Ann. Tech. Conf. Proceedings (Society of Vacuum Coaters), 1999, p. 456.
[4]M. S. Weaver *et al.*, Appl. Phys. Lett. **81**, 2929 (2002).
[5]A. Chwang *et al.*, Appl. Phys. Lett. **83**, 413 (2003).
[6]G. Nisato and Y. Leterrier, Mater. Res. Soc. Symp. Proc. **769**, H1.4 (2003).
[7]H. Chatham, Surf. Coat. Technol. **78**, 1 (1996).
[8]W. Decker and B. M. Henry, 45th Ann. Tech. Conf. Proceedings (Society of Vacuum Coaters), 2002, p. 492.
[9]A. S. da Silva Sobrinho, M. Latreche, G. Czeremuszkin, J. E. Klemberg-Sapieha, and M. R. Wertheimer, J. Vac. Sci. Technol. A **16**, 3190 (1998).
[10]A. S. da Silva Sobrinho, G. Czeremuszkin, M. Latreche, and M. R. Wertheimer, J. Vac. Sci. Technol. A **18**, 149 (2000).
[11]A. G. Erlat, R. J. Spontak, R. P. Clarke, T. C. Robinson, P. D. Haaland, Y. Tropsha, N. G. Harvey, and E. A. Vogler, J. Phys. Chem. B **103**, 6047 (1999).
[12]R. M. Barrer, *Diffusion In and Through Solids* (Cambridge University

Press, New York, 1941).
[13]B. E. Deal and A. S. Grove, J. Appl. Phys. **36**, 3770 (1965).
[14]E. H. H. Jamieson and A. H. Windle, J. Mater. Sci. **18**, 64 (1983).
[15]Y. G. Tropsha and N. G. Harvey, J. Phys. Chem. B **101**, 2259 (1997).
[16]M. Schaepkens, T. W. Kim, A. G. Erlat, M. Yan, K. W. Flanagan, C. M. Heller, and P. A. McConnelee, J. Vac. Sci. Technol. A **22**, 1716 (2004).
[17]A. P. Roberts, B. M. Henry, A. P. Sutton, C. R. M. Grovenor, G. A. D. Briggs, T. Miyamoto, M. Kano, Y. Tsukahara, and M. Yanaka, J. Membr. Sci. **208**, 75 (2002).
[18]M. S. Weaver *et al.*, Appl. Phys. Lett. **81**, 2929 (2002).
[19]G. Nisato, M. Kuilder, P. Bouten, L. Moro, O. Philips, and N. Rutherford, Society for Information Display, 2003 International Symposium, Digest of Technical Papers, 2003, Vol. XXXIV, p. 88.
[20]L. Moro, T. A. Krajeweski, N. M. Rutherford, O. Philips, R. J. Visser, M. E. Gross, W. D. Bennett, and G. L. Graff, Proc. SPIE **5214**, 83 (2004).
[21]J. S. Lewis and M. S. Weaver, IEEE J. Sel. Top. Quantum Electron. **10**, 45 (2004).
[22]G. L. Graff, R. E. Williford, and P. E. Burrows, J. Appl. Phys. **96**, 1840 (2004).
[23]E. H. Nicollian and J. R. Brews, *MOS Physics and Technology* (Wiley, New York) Chap. 16.
[24]A. S. da Silva Sobrinho, N. Schuhler, J. E. Klemberg-Sapieha, M. R. Wertheimer, M. Andews, and S. C. Gujrathi, J. Vac. Sci. Technol. A **16**, 2021 (1998).
[25]G. Nisato, P. C. P. Bouten, P. J. Slinkkerveer, W. D. Bennet, G. L. Graff, N. Rutherford, and L. Wiese, Asia Display/IDW Proc., 2001.
[26]P. O. Nilsson and G. Forsell, Phys. Rev. B **16**, 3352 (1977).
[27]R. Paetzold, A. Winnacker, D. Henseler, V. Cesari, and K. Heuser, Rev. Sci. Instrum. **74**, 5147 (2003).
[28]A. G. Erlat, M. Schaepkens, T. W. Kim, C. M. Heller, M. Yan, and P. McConnelee, 47th Ann. Tech. Conf. Proceedings (Society of Vacuum Coaters), 2004 (in press).